Numerical Simulation of Intrinsic Bistability and High-Frequency Current Oscillations in Resonant Tunneling Structures

K. L. Jensen and F. A. Buot
Naval Research Laboratory, Washington, D.C. 20375-5000
(Received 17 September 1990)

Intrinsic high-frequency oscillations (≈ 2.5 THz) in current and corresponding quantum-well density have been simulated for the first time for a fixed-bias voltage in the negative differential resistance (NDR) region of the current-voltage (I-V) characteristics of a resonant tunneling diode. Scattering and self-consistency are included. Hysteresis and "plateaulike" behavior of the time-averaged I-V curve are simulated in the NDR region. Intrinsic bistability is manifested by the phenomenon of unstable electron charge buildup and ejection from the quantum well.

PACS numbers: 73.40.Gk

The resonant tunneling of electrons through double-barrier structures is known to produce a region of negative differential resistance (NDR) in the I-V relationship. This has been well established experimentally,[1-5] and a simple understanding of the phenomena may be obtained through analyzing the transmission coefficient of the one-dimensional resonant tunneling diode (RTD) profile.[6-9] Transmission-coefficient-based calculations can include self-consistency and duplicate gross features of RTD I-V curves, but they are impractical for simulating time-dependent nonlinear effects, such as occur when the bias is suddenly switched (transient response or frequency-dependent behavior) and other time-dependent nonlinear phenomena such as the high-frequency oscillations at fixed bias in the NDR region simulated in this paper.

As the full characterization of RTD devices requires simulating a time-evolving system, the Wigner distribution function[10] (WDF) approach has emerged as the most promising method.[11-15] Scattering within the device and self-consistency[13,15-17] may be included, and the WDF approach has the added advantage of lending itself to a "particle" interpretation.[15,16,18] We present here a more accurate and fully time-dependent and self-consistent quantum transport simulation[15] which includes scattering as a function of temperature and which demonstrates current oscillations at a fixed bias. We note, however, that other time-dependent and self-consistent scattering calculations have been reported prior to the current work,[12-14] but they differ from ours in some key respects.[19] The method we have chosen to incorporate self-consistency and scattering allows us to address more accurately the controversial "bistability" issue reported[4,20] and challenged[21] previously.

The experimentally reported I-V curves exhibit a characteristic "plateaulike" behavior[5,22] and hysteresis.[20,21] The first view proposed by Goldman, Tsui, and Cunningham[4] attributed this entire behavior to "intrinsic bistability," that is, charge is dynamically built up and ejected from the well, and through an electrostatic feedback mechanism, two current states exist. Sollner,[21] who represents the second view, disagrees, claiming that instead of Goldman's hysteresis being due to a charging of the well, it is due to external circuit-induced oscillations of the current in the NDR region of the device. We have observed intrinsic oscillations (which have a frequency of roughly 2.5 THz) in the current density in the NDR region, but not elsewhere along the I-V curve, and these oscillations are due to a nontrivial interaction between the electron density (and hence, the self-consistent potential) and the transmission properties of the RTD. We have also observed dynamical bistability manifested by an unstable buildup of electrons in the well when the bias is swept in the positive direction, and an unstable depletion of electrons when the bias is swept in the reverse direction.

The parameters we used are similar to or the same as those used previously.[17,23] Momentum and position space are broken up into 72 and 86 points, respectively. The electron density is 2×10^{18} particles/cm^3; the compensation ratio for scattering calculations is 0.3; the barrier and well widths are 30 and 50 Å; the simulation region is 550 Å; the potential barriers are 0.3 eV, corresponding to $Al_{0.3}Ga_{0.7}As$; the temperature is 77 K; the transient time step is 1 fs; a second-order differencing scheme (SDS) is used to approximate the spatial derivative, and the Cayley form of the time-evolution operator is used; the effective mass of the electron is assumed to be constant across the device and equal to $0.0667m_0$; the doping extends to 30 Å before the first barrier and after the second; the quantum-well region (170 Å) is undoped. Relaxation time calculations use bulk GaAs parameters and the chemical potential is found by requiring that $\int_0^\infty \sqrt{\varepsilon} f(\varepsilon)\,d\varepsilon = \frac{2}{3}\mu(T=0)^{3/2}$, where $f(\varepsilon)$ is the Fermi distribution.[17] Dissipation is due to scattering within the device and the open boundary condition.

A self-consistent equilibrium distribution is obtained by starting with a neutral charge distribution and then allowing the system to time evolve by simultaneously solving the one-dimensional Poisson equation at each time step to obtain a self-consistent potential profile to calculate the WDF for the next time step, to an equilibrium state for a particular doping profile.[24] The WDF calculated at one bias is then used as the starting point

Work of the U. S. Government
Not subject to U. S. copyright

for finding the WDF at the next bias step. Because convergence to steady state takes as long as 1000 time steps or more, obtaining the current over a range of biases can prove time consuming, even though one time step on a Cray X-MP computer for the parameters used here takes less than 3.2 s of CPU time.[25] Accelerated convergence can be achieved with some ingenuity. Near steady state, the potential does not change significantly; therefore, a number of time steps may be taken with the potential held fixed before a self-consistent correction is made. Therefore, by running the simulation in time increments of typically 50 fs before a self-consistent correction to the potential is made, and then taking the average of the initial and final distributions as a new starting distribution for the next increment, the CPU time for convergence is decreased by an order of magnitude. This "accelerated convergence technique" (ACT) achieves the steady-state WDF in a fraction of the CPU time that would be required if the potential were self-consistently calculated per time step (the "natural" or physically based approach); to obtain the correct steady-state distribution, the final ACT state is then further time evolved in the natural manner to ensure that the current across the device remains uniform across the device and constant over time.

In the NDR region, however, ACT fails to give a current which is uniform across the device and constant in time. Indeed, unlike the non-NDR biases, the final ACT current calculated for an NDR bias has a standard deviation which will grow (within limits) when the natural time evolution is then performed on the distribution obtained from ACT. This represented our first clue that oscillations in the current exist in the NDR region. To get the NDR currents, we used only the natural time-evolution approach and performed 1600 time steps per point on the I-V curve (double this amount at the end points on the hysteresis loop). For the parameters we used, the oscillations occur for biases between 0.23 and 0.32 V.

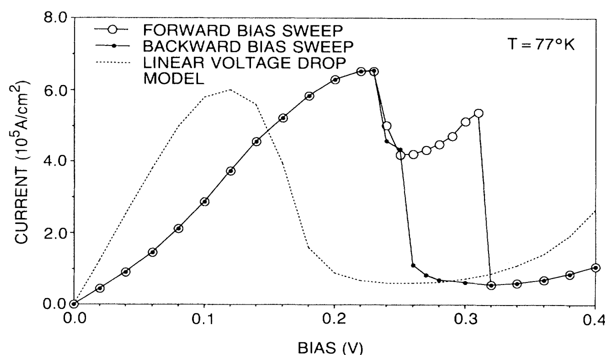

FIG. 1. Current as a function of applied bias. "Linear drop" refers to (non-self-consistent) simulations in which the bias was assumed to linearly decrease across the quantum-well region (Ref. 23). The NDR region occurs between biases of 0.23 and 0.32 V.

The current evaluated in the NDR region is dependent on the direction in which the bias voltage is swept from the non-NDR regions. Starting from two distributions which have uniform and constant currents on opposite sides of the NDR region (0.18 and 0.35 V were the starting biases, Fig. 1), the bias is then incrementally increased (in the case of 0.18 V) or decreased (in the case of 0.35 V) and allowed to come to steady state naturally before the next bias increment is performed; the increments in bias were taken to be 0.01 V. The decreasing bias simulations gave small currents which were uniform across the device and constant for almost all biases in the NDR region, before dynamical bistability sets in. For the increasing bias simulations, however, the NDR region was characterized by more or less periodic oscillations (Figs. 2 and 3) in the current magnitude at the drain end (since the source and drain ends have the same time-averaged currents, we chose to concentrate on the drain currents). The period of the oscillations was typically between 200 and 400 fs and the magnitude varied by as much as 1×10^5 A/cm^2, though the oscillating current for the increasing bias sweep takes on values considerably larger than the current obtained in the decreasing bias simulations when the former is oscillating and the latter is not. To calculate the I-V points in the NDR region, the time-evolving current was averaged over several periods of oscillation. The averaged currents in the increasing bias simulations form the characteristic experimental plateaulike structure in the NDR region.

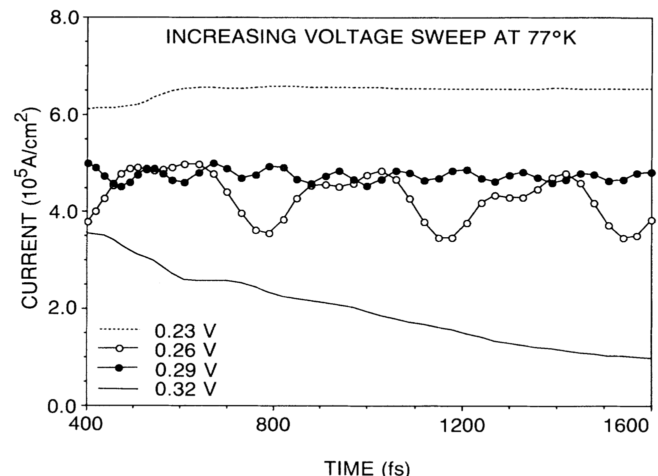

FIG. 2. Time evolution of the current for various biases for the increasing-bias sweep points. At time $t=0$ fs, the voltage is increased by 0.01 V. The initial WDF is given by the steady-state distribution of the previous bias step. For a bias of 0.23 V, the current settles to a constant value. For biases up to 0.31 V, the current is oscillatory, and at 0.32 V, the current initially oscillates with an average value of 5.3×10^5 A/cm^2 but decays into a nonoscillatory state with a value of 7×10^4 A/cm^2 over a time scale on the order of 2000 fs (the bistable case).

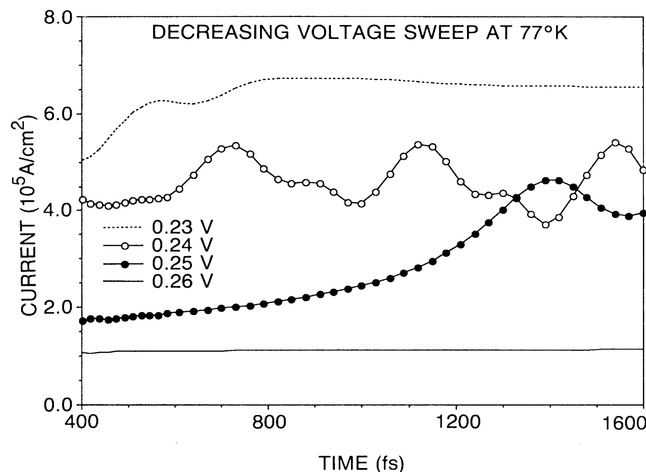

FIG. 3. Time evolution of the current for various biases for the decreasing-bias sweep points. The current for biases above 0.25 V is numerically constant and uniform, but at 0.25 V, the current initially is nonoscillatory but slowly increases until it becomes oscillatory over a time scale on the order of 800 fs. Only for biases of 0.25 and 0.24 V does the current oscillate; for 0.23 V, the value of the current becomes constant and equal to the current for the increasing-bias sweep case. The bistable case occurs for 0.25 V.

The nonuniformity of the current and the oscillations themselves are correlated with the filling and depletion of the electron density in the well, and are similar to the oscillations observed after a sudden bias switch when a linear bias voltage drop was assumed;[17] however, these switched-bias oscillations rapidly relax over time and became insignificant after 500 fs. The present fixed-bias oscillations, on the other hand, seem to be driven by the self-consistency, similar to plasma oscillations, and show a steady amplitude over the relatively long time of the simulation (1600 fs). For two *I-V* points (decreasing at 0.25 V, increasing at 0.32 V), the time-dependent current went from a nonoscillatory state to a higher current oscillating one and vice versa (Figs. 2 and 3). This demonstrated for the first time a dynamical intrinsic bistability at these bias conditions. This is also manifested in the bistable charging condition of the quantum well (Figs. 4 and 5); indeed, the shape of a plot of the calculated charge stored in the quantum well is very similar to Fig. 1. The dynamical bistability occurs only at 0.25 and 0.32 V in the NDR region, resulting in the overall hysteresis behavior in the *I-V* characteristics.

Previous theoretical works[26] which address the question of bistability in the RTD deal only either with charge-storage effects in the quantum well or with externally induced high-frequency oscillating currents in the NDR region. Notably, Kluksdahl *et al.*, using a WDF approach, failed to see the intrinsic high-frequency oscillating effects in the NDR region for a fixed bias and therefore attributed bistability as solely due to charge-storage effects within the quantum well. Our results

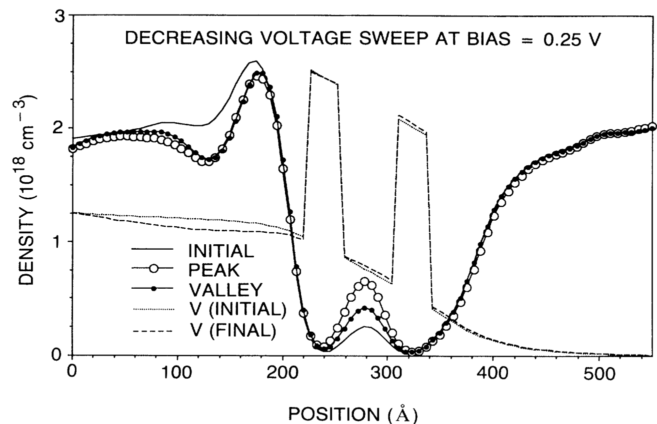

FIG. 4. Density as a function of position for various times at a bias of 0.25 V for the decreasing sweep. "Initial" corresponds to the density when the current is in the nonoscillatory regime. "Peak" and "valley" are the electron-density profiles corresponding to the current when it is in the oscillatory regime and at its maximum and minimum values, respectively (see Fig. 2). "*V*(initial)" refers to the self-consistent potential in the initial state and "*V*(final)" refers to the oscillating state.

show that the intrinsic oscillations have a dominant influence on the shape of the plateaulike structure and hysteresis in the *I-V* characteristics. The current work reports for the first time a direct numerical observation of high-frequency oscillations for a fixed bias, whereas previous work,[14] including ours,[15-18,23] observed the oscillations in the transient response to a sudden bias shift. The presence of the oscillations is temperature dependent: At 300 K with scattering included in the device,

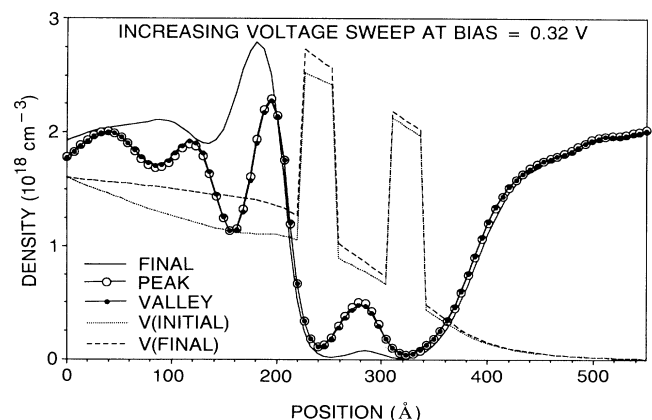

FIG. 5. Density as a function of position for various times at a bias of 0.32 V for the increasing sweep. "Final" corresponds to the density when the current is in the nonoscillatory regime. "Peak" and "valley" are the electron-density profiles corresponding to the current when it is in the oscillatory regime and at its maximum and minimum values, respectively (see Fig. 3). "*V*(initial)" refers to the potential in the oscillating state and "*V*(final)" refers to the initial state.

oscillations and a hysteresis loop were not observed for the RTD parameters simulated. We believe that ballistic (no scattering) calculations would show larger oscillations and hysteresis loops.

In conclusion, our simulation shows that intrinsic high-frequency current oscillations lead to the characteristic plateaulike *I-V* behavior for an increasing voltage sweep and that charging of the well at some bias voltages leads to dynamic current bistability in the *I-V* characteristic of the resonant tunneling structures. Both of these effects lead to the experimentally found hysteresis behavior of the *I-V* curve. A full quantitative analysis of the physical transport processes in the RTD responsible for the high-frequency oscillations is underway. Presently, it seems that the RTD operating in the NDR region behaves similar to an equivalent circuit consisting of a resistor in series with a two-branch parallel circuit with one branch consisting of a capacitor and the other consisting of an inductor and a negative resistor. The parameters for this circuit were extracted from the RTD simulations and the circuit does indeed oscillate for a fixed bias in the NDR. From our preliminary results we believe that the inductance is due to a phase delay caused by a correlation between the self-consistent resonant energy level and the incoming electron energies from the source region; i.e., charge accumulation in the well tends to align the Fermi level of the source with the resonant energy level as time evolved, resulting in an inductive delay. A full analysis of the detailed quantum transport physical processes involved in this phenomena will be given in a separate paper, and will address the inductance aspects of the RTD transport processes in the NDR region.

The authors are grateful for stimulating discussions on experimental results and setups with Dr. H. Newman, Dr. S. Kirchoffer, and Dr. R. Magno. This work was supported by the Office of Naval Research and the Office of Naval Technology.

[1]L. L. Chang, L. Esaki, and R. Tsu, Appl. Phys. Lett. **24**, 593 (1974).

[2]T. J. Shewchuk, P. C. Chapin, P. D. Colman, W. Kopp, R. Fischer, and H. Morkoc, Appl. Phys. Lett. **48**, 508 (1985).

[3]M. A. Reed, J. W. Lee, and H-L. Tsai, Appl. Phys. Lett. **49**, 159 (1986).

[4]V. J. Goldman, D. C. Tsui, and J. E. Cunningham, Phys. Rev. Lett. **58**, 1256 (1987).

[5]P. Gueret, C. Rossel, E. Marclay, and H. Meier, J. Appl. Phys. **66**, 278 (1989).

[6]K. M. S. V. Bandara and D. D. Coon, J. Appl. Phys. **66**, 693 (1989).

[7]D. Landheer and G. C. Aers, Superlattices Microstruct. **7**, 17 (1990).

[8]M. Cahay, M. McLennan, S. Datta, and M. S. Lundstrom, Appl. Phys. Lett. **50**, 612 (1987).

[9]C. M. Tan, J. Xu, and S. Zukotynski, J. Appl. Phys. **67**, 3011 (1990).

[10]For an excellent treatment of the Wigner distribution function, see V. I. Tatarskii, Usp. Fiz. Nauk **139**, 587 (1983) [Sov. Phys. Usp. **26**, 311 (1983)].

[11]J. Barker, Physica (Amsterdam) **134B**, 22 (1985).

[12]W. R. Frensley, Phys. Rev. B **36**, 1570 (1987).

[13]W. R. Frensley, Solid State Electron. **31**, 739 (1988).

[14]N. C. Kluksdahl, A. M. Kriman, D. K. Ferry, and C. Ringhofer, Phys. Rev. B **39**, 7720 (1989); N. C. Kluksdahl, A. M. Kriman, and D. K. Ferry, Solid State Electron. **32**, 1273 (1989).

[15]F. A. Buot and K. L. Jensen, Phys. Rev. B **42**, 9429 (1990).

[16]K. L. Jensen and F. A. Buot, "The Methodology of Simulating Particle Trajectories Through Tunneling Structures Using a Wigner Distribution Approach," Proceedings of the Third International Vacuum Microelectronics Conference, Monterey, CA, 23–25 July 1990 [IEEE Trans. Electron Devices Pt. II (to be published)].

[17]K. L. Jensen and F. A. Buot, J. Appl. Phys. **67**, 7602 (1990).

[18]K. L. Jensen and F. A. Buot, Appl. Phys. Lett. **55**, 669 (1989).

[19]In Frensley's work (Ref. 12) calculation of the *I-V* is based on solving for the time-independent WDF coupled to Poisson's equation in one large matrix equation, then iterating the solution to convergence. In Kluksdahl *et al.* (Ref. 14) they have performed time-dependent self-consistent calculations and have examined bistability in the *I-V* curves for RTD's at 300 K; however, the relaxation-time collision operator and numerical methods used for time evolving the WDF differ from ours.

[20]A. Zaslavsky, V. J. Goldman, D. C. Tsui, and J. E. Cunningham, Appl. Phys. Lett. **53**, 1409 (1988).

[21]T. C. L. G. Sollner, Phys. Rev. Lett. **59**, 1622 (1987).

[22]This plateau region is also apparent in InAs/AlSb structures: J. R. Soderstrom, D. H. Chow, and T. C. McGill, IEEE Electron Device Lett. **11**, 27 (1990).

[23]K. L. Jensen and F. A. Buot, J. Appl. Phys. **67**, 2153 (1990).

[24]This is a standard approach in a fully time-dependent device simulation. See, for example, F. A. Buot, Compel **6**, 45 (1987).

[25]This represents over an order-of-magnitude improvement in the efficiency of calculating the WDF as compared to the results reported in Ref. 15; it is due to an improved vectorization of the code and the use of more recent International Mathematics and Scientific Library (IMSL) (version 10) routines.

[26]F. W. Sheard and G. A. Toombs, Appl. Phys. Lett. **52**, 1228 (1988); J. F. Young, B. M. Wood, H. C. Liu, M. Buchanan, and D. Landheer, Appl. Phys. Lett. **52**, 1398 (1988); H. C. Liu, Appl. Phys. Lett. **53**, 485 (1988); R. K. Mains, J. P. Sun, and G. I. Haddad, Appl. Phys. Lett. **55**, 371 (1989); T. Baba and M. Mizuta, Jpn. J. Appl. Phys. Pt. 2, **28**, L1322 (1989).